

Supporting Information for:

# Radical Reactivity of the Fe(III)/Fe(II) Tetramesitylporphyrin Couple: Hydrogen Atom Transfer, Oxyl Radical Dissociation, and Catalytic Disproportionation of a Hydroxylamine

Thomas R. Porter, James M. Mayer\*

University of Washington, Department of Chemistry, Box 351700, Seattle, Washington  
mayer@chem.washington.edu

## Contents:

|                                                                                                                                                          |     |
|----------------------------------------------------------------------------------------------------------------------------------------------------------|-----|
| 1. BDFE calculations using Abraham's Model .....                                                                                                         | S2  |
| 2. $^1\text{H}$ NMR spectrum of $(\text{TMP})\text{Fe}^{\text{III}}(\text{OH}) + \frac{1}{2} \text{PhHNHNPh}$ .....                                      | S3  |
| 3. $^1\text{H}$ NMR spectrum of $(\text{TMP})\text{Fe}^{\text{III}}(\text{OH}) + \frac{1}{2} \text{PhHNH}_2$ .....                                       | S4  |
| 4. Stopped-Flow kinetics of $(\text{TMP})\text{Fe}^{\text{III}}(\text{OH}) + \text{TEMPOH}$ .....                                                        | S5  |
| 5. Calculation of $K_4$ of $(\text{TMP})\text{Fe}^{\text{II}} + \text{TEMPO}$ using NMR data .....                                                       | S6  |
| 6. van't Hoff analysis of $(\text{TMP})\text{Fe}^{\text{II}} + \text{TEMPO}$ using variable temperature optical data .....                               | S8  |
| 7. Decoalescence of $(\text{TMP})\text{Fe}^{\text{III}}(\text{TEMPO})$ <i>m</i> -aryl peaks in variable temperature NMR spectra                          | S10 |
| 8. $^1\text{H}$ NMR spectrum of $(\text{TMP})\text{Fe}^{\text{II}} + \text{substoichiometric TEMPO at } -80^\circ\text{C}$ .....                         | S12 |
| 9. $^1\text{H}$ NMR spectrum of $(\text{TMP})\text{Fe}^{\text{III}}('Bu_3\text{ArO}) + \text{H}_2\text{O}$ .....                                         | S13 |
| 10. $^1\text{H}$ NMR spectrum of $(\text{TMP})\text{Fe}^{\text{II}} + \text{TEMPOH}$ .....                                                               | S14 |
| 11. $^1\text{H}$ NMR spectrum of $(\text{TMP})\text{Fe}^{\text{II}} + 2 \text{TEMPOH}$ .....                                                             | S15 |
| 12. Kinetic data for the catalytic disproportionation of TEMPOH in the presence of catalytic $(\text{TMP})\text{Fe}^{\text{II}}$ .....                   | S16 |
| 13. Mass balance plot for the disproportionation of TEMPOH in the presence of catalytic $(\text{TMP})\text{Fe}^{\text{II}}$ .....                        | S17 |
| 14. Experimental details for the treatment of $(\text{TMP})\text{Fe}^{\text{III}}(\text{OH})$ with excess P1-phosphazene $\text{H}^+\text{BF}_4^-$ ..... | S18 |

## 1. BDFE calculations using Abraham's Model

The interconversion between solution BDFEs ( $\text{BDFE}_{\text{solv}}$ ) of different hydrogen atom transfer reagents can be achieved by first converting  $\text{BDFE}_{\text{solv}}$  to a gas phase BDFE ( $\text{BDFE}_g$ ) by accounting for the free energy of solvation of  $\text{H}^\bullet$  and the difference in free energy of solvation of  $\text{XH}$  and  $\text{X}^\bullet$  (Eqn 1).<sup>1</sup> The reported BDFE values of 1,2-diphenylhydrazine and phenylhydrazine in DMSO are 67.1 and 70.3 kcal mol<sup>-1</sup>, respectively.<sup>1</sup>

$$(1) \text{BDFE}_{\text{solv}} = \text{BDFE}_g + \Delta G^\circ_{\text{solv}}(\text{H}^\bullet) + [\Delta G^\circ_{\text{solv}}(\text{X}^\bullet) - \Delta G^\circ_{\text{solv}}(\text{XH})]$$

$\Delta G^\circ_{\text{solv}}(\text{H}^\bullet)$  can be calculated from the solubility of  $\text{H}^\bullet$  (assumed to be the same as  $\text{H}_2$ <sup>1</sup>) at STP in different solvents (Eqn 2).  $\Delta G^\circ_{\text{solv}}(\text{H}^\bullet)$  in toluene is 4.77 kcal mol<sup>-1</sup> and  $\Delta G^\circ_{\text{solv}}(\text{H}^\bullet)$  in DMSO is 5.61 kcal mol<sup>-1</sup>.<sup>2,3</sup>

$$(2) \Delta G^\circ_{\text{solv}}(\text{H}^\bullet) = -RT\ln(K_{\text{sol}})$$

In aprotic solvents, the  $[\Delta G^\circ_{\text{solv}}(\text{X}^\bullet) - \Delta G^\circ_{\text{solv}}(\text{XH})]$  term is taken as the free energy of the  $\text{XH}$ -solvent hydrogen bond. This can be calculated using empirically determined H-bonding acidity ( $\alpha_2^{\text{H}}$ ) and basicity parameters ( $\beta_2^{\text{H}}$ ) described by Abraham (Eqn. 3).

$$(3) \Delta G^\circ_{\text{solv}} = -10.02\alpha_2^{\text{H}}\beta_2^{\text{H}} - 1.492$$

The  $\beta_2^{\text{H}}$  parameter in DMSO is 0.78 and in toluene is 0.14.<sup>4</sup> The  $\alpha_2^{\text{H}}$  value of 1,2-diphenylhydrazine or phenylhydrazine is not reported but an estimate of 0.3 can be made for both by comparison to other reported N-H compounds (diphenylamine  $\alpha_2^{\text{H}} = 0.324$ , aniline = 0.264, and 3-chloroaniline = 0.33).<sup>5</sup>

Combining these equations, the BDFE values of 1,2-diphenylhydrazine and phenylhydrazine reported in DMSO can be converted to BDFE values in toluene.

$$(4) \text{BDFE}_{\text{tol}} = \text{BDFE}_{\text{DMSO}} - [\Delta G^\circ_{\text{solv}}(\text{H}^\bullet)_{\text{DMSO}} - \Delta G^\circ_{\text{solv}}(\text{XH})_{\text{DMSO}}] + [\Delta G^\circ_{\text{solv}}(\text{H}^\bullet)_{\text{tol}} - \Delta G^\circ_{\text{solv}}(\text{XH})_{\text{tol}}]$$

Converting the reported BDFE values for 1,2-diphenylhydrazine and phenylhydrazine in DMSO to BDFE values in toluene using this model give values of  $64.3 \pm 1.5$  and  $67.6 \pm 1.5$  kcal mol<sup>-1</sup>, respectively.

A more complete description of the use of Abraham's model of interconverting solution BDFE values can be found in reference 4.

- (1) J. J. Warren, T. A. Tronic, J. M. Mayer, *Chem. Rev.*, 2010, **110**, 7062.
- (2) E. J. Brunner, *J. Chem. Eng. Data*, 1985, **30**, 269.
- (3) E. A. Symons, *Can. J. Chem.*, 1971, **49**, 3940.

- (4) J. J. Warren, J. M. Mayer, *Proc. Natl. Acad. Sci.* 2010, **107**, 5282.
- (5) M. H. Abraham, P. L. Grellier, D. V. Prior, P. P. Duce, *J. Chem. Soc. Perkin Trans. II*, 1989, 699.

2.  $^1\text{H}$  NMR spectrum of (TMP)Fe<sup>III</sup>(OH) +  $\frac{1}{2}$  PhNHNHPh

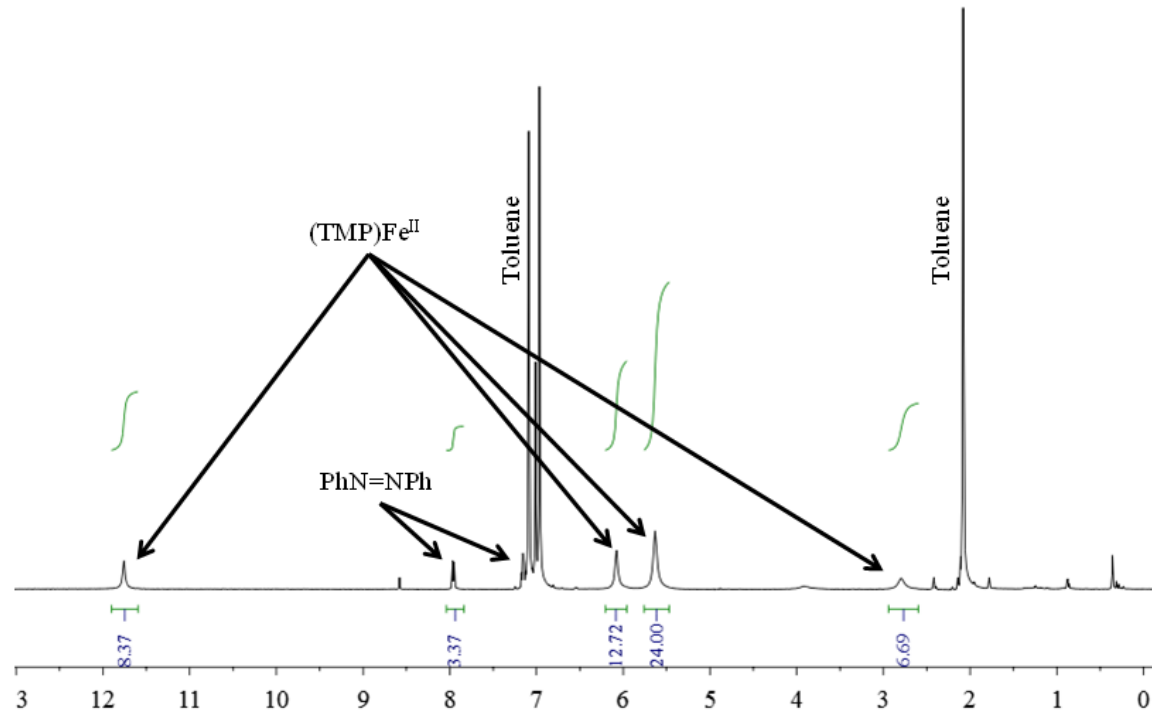
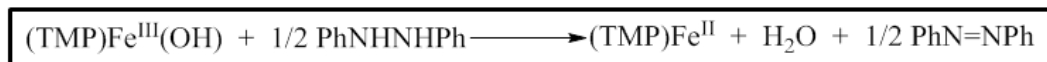


Figure S1  $^1\text{H}$  NMR spectrum of the reaction mixture of (TMP)Fe<sup>III</sup>(OH) and 0.5 equiv hydrazobenzene in toluene- $d_8$  after 6 hours.

### 3. $^1\text{H}$ NMR spectrum of (TMP)Fe<sup>III</sup>(OH) + ½ PhNHNH<sub>2</sub>

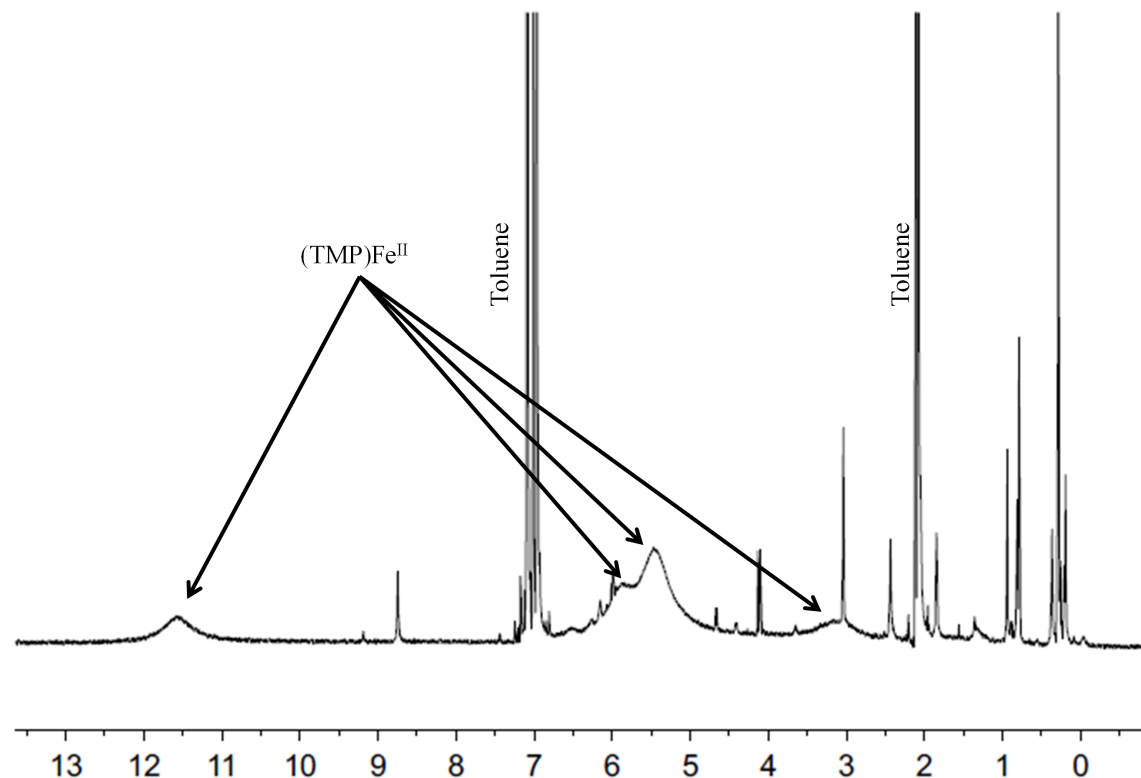


Figure S2.  $^1\text{H}$  NMR spectrum of the reaction mixture of (TMP)Fe<sup>III</sup>(OH) and 0.5 equiv phenylhydrazine in toluene- $d_8$  after 10 hours.

The  $^1\text{H}$  NMR spectrum of the reaction mixture containing (TMP)Fe<sup>III</sup>(OH) and 0.5 equivalents of phenylhydrazine resulted in the generation of (TMP)Fe<sup>II</sup> and presumably H<sub>2</sub>O and PhN=NH. PhN=NH is known to decompose readily<sup>6</sup> to multiple products and was not observed.

(6) P.-K. Huang, E. M. Kosower, *J. Am. Chem. Soc.*, 1968, **90**, 2367.

#### 4. Stopped-Flow kinetics of (TMP)Fe<sup>III</sup>(OH) + TEMPOH

Toluene solutions were prepared and loaded into gas tight syringes fitted with gas tight valves in a nitrogen filled glovebox before being affixed to an OLIS RMS-1000 spectrophotometer. Measurements were taken at 25°C. Reactions were performed under pseudo-first order conditions (80 μM (TMP)Fe<sup>III</sup>(OH), 3.6–14.4 mM TEMPOH). Data were fit by the SPECFIT/32<sup>TM</sup> global analysis program to a simple first order model and a second order rate constant was determined.

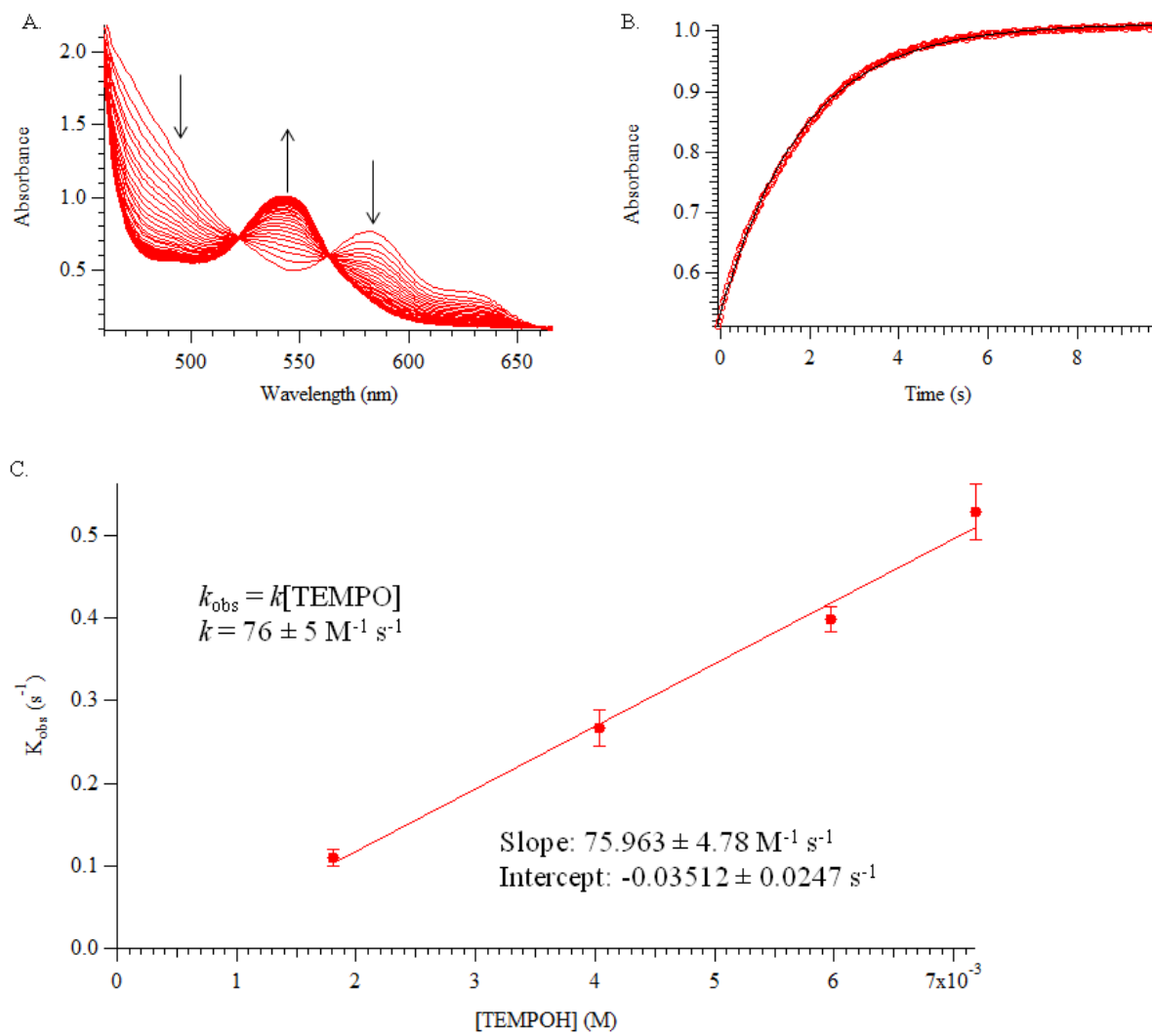


Figure S3. **A.** Spectra of the reaction of (TMP)Fe<sup>III</sup>(OH) with TEMPOH *vs.* time. **B.** Kinetic trace of the reaction at 525 nm (red markers) and fit (black line). **C.** Pseudo-first order plot of  $k_{\text{obs}}$  *vs.* [TEMPOH].

## 5. Calculation of $K_4$ of (TMP)Fe<sup>II</sup> + TEMPO using NMR data

Chemical shifts of “pure” (TMP)Fe<sup>III</sup>(TEMPO) were estimated by plotting  $\delta_{\text{obs}}$  vs. [TEMPO] and extrapolating to infinite TEMPO concentration. This is shown for the *m*-ArH, *o*-ArCH<sub>3</sub>, and  $\beta$ -pyrrolic resonances in Figure S4.

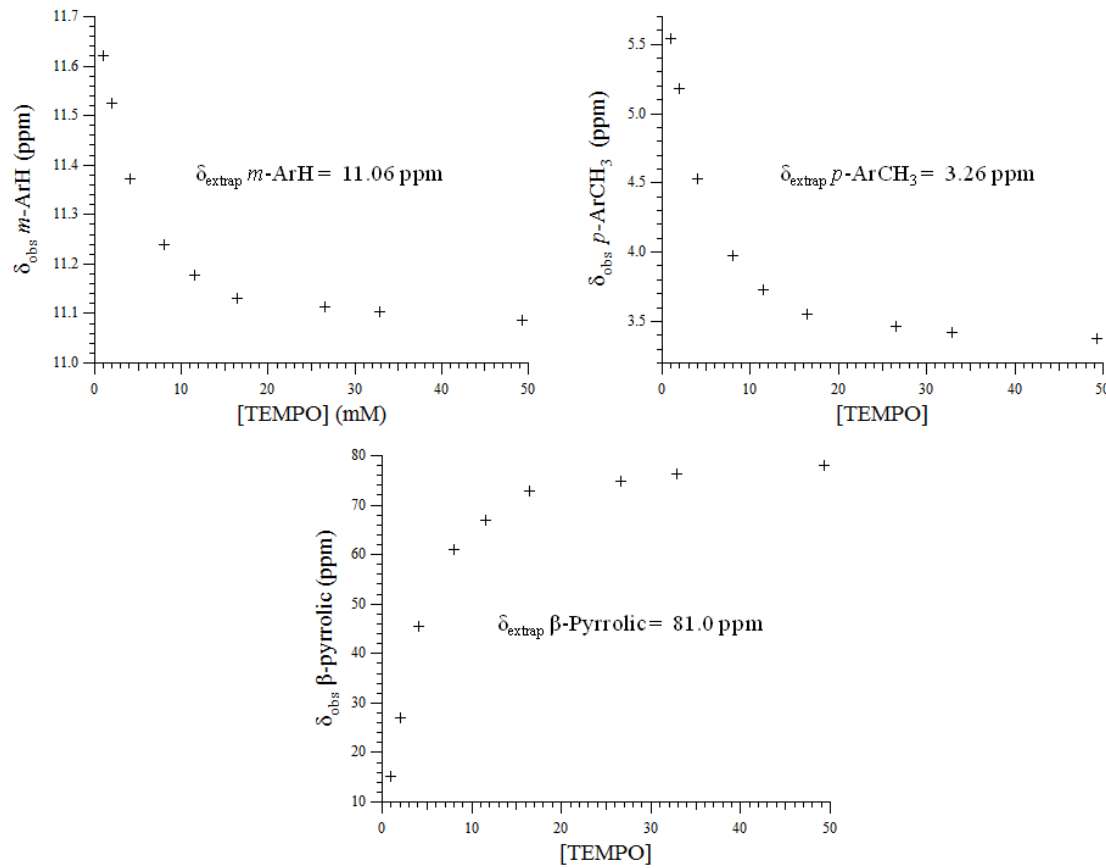


Figure S4. Plots of the observed chemical shift of (TMP)Fe<sup>II</sup>/(TMP)Fe<sup>III</sup>(TEMPO) vs. concentration of TEMPO. Values of “pure” (TMP)Fe<sup>III</sup>(TEMPO) are determined by extrapolating to infinite [TEMPO].

Using mass balance assumptions, the equilibrium concentrations of (TMP)Fe<sup>II</sup>, (TMP)Fe<sup>III</sup>(TEMPO) (abbreviated Fe<sup>II</sup> and Fe<sup>III</sup>), and TEMPO were calculated using the following expressions.

$$[\text{Fe}^{\text{II}}] = [\text{Fe}^{\text{II}}_0] (\delta_{\text{obs}} - \delta_{\text{Fe(III)}})/(\delta_{\text{Fe(II)}} - \delta_{\text{Fe(III)}})$$

$$[\text{Fe}^{\text{III}}] = [\text{Fe}^{\text{II}}_0] - [\text{Fe}^{\text{II}}]$$

$$[\text{TEMPO}] = [\text{TEMPO}_0] - [\text{Fe}^{\text{III}}]$$

$[Fe^{II}]$  is the equilibrium concentration of  $Fe^{II}$ ,  $[Fe^{II}_0]$  is the initial concentration of  $Fe^{II}$ ,  $\delta_{obs}$  is the observed chemical shift,  $\delta_{Fe(III)}$  is the extrapolated chemical shift of  $Fe^{III}$ ,  $\delta_{Fe(II)}$  is the chemical shift of  $Fe^{II}$ , and  $[TEMPO_0]$  is the initial concentration of TEMPO.

Plotting  $[Fe^{III}]/[Fe^{II}]$  vs.  $[TEMPO]$  gives a linear fit that goes through the origin. The slope is the equilibrium constant:  $K_4 = 520 \pm 25 M^{-1}$ .

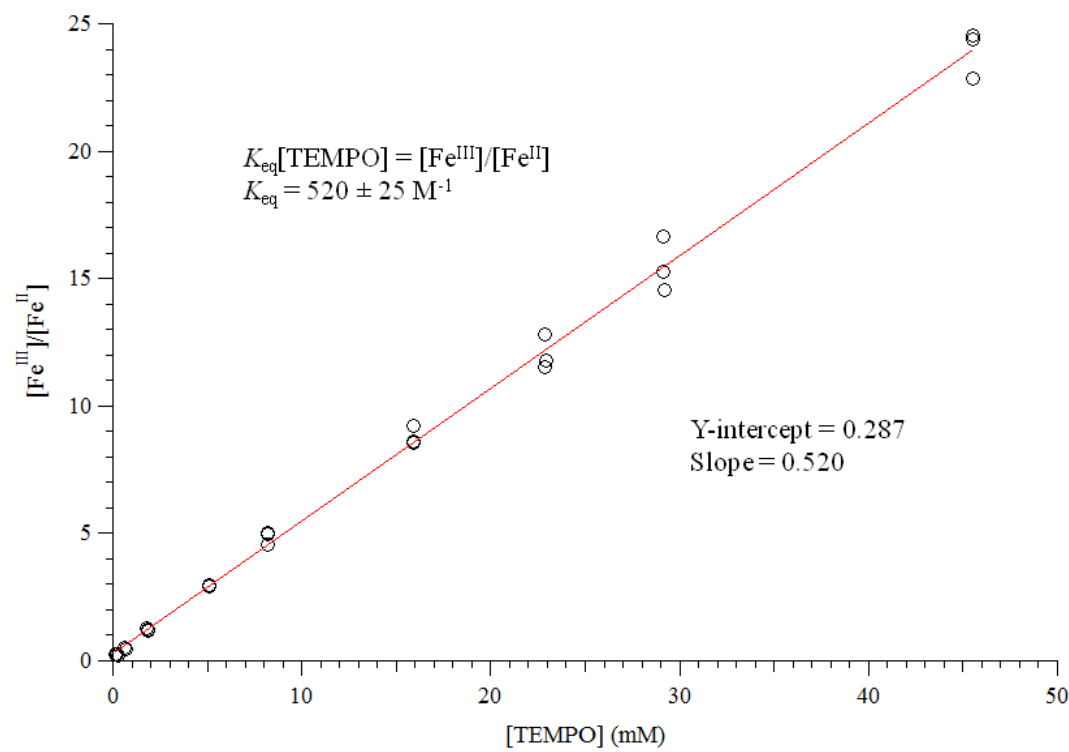


Figure S5. Plot of  $[(TMP)Fe^{II}]/[(TMP)Fe^{III}(TEMPO)]$  vs.  $[TEMPO]$  from  $^1H$  NMR spectra. The slope is  $K_4$ .

## 6. van't Hoff analysis of (TMP)Fe<sup>II</sup> + TEMPO using variable temperature optical data.

The epsilon values of “pure” (TMP)Fe<sup>III</sup>(TEMPO) were measured by preparing a sample of 80 μM (TMP)Fe<sup>II</sup> in toluene with 5 equivalents of TEMPO. Optical spectra were taken as the temperature was lowered. When the temperature was decreased below approximately –50 °C, no additional spectral changes were observed. The absorption spectrum observed in this temperature independent regime was taken to be that of “pure” (TMP)Fe<sup>III</sup>(TEMPO). The epsilon values of (TMP)Fe<sup>III</sup>(TEMPO) from three different wavelengths were used to calculate equilibrium concentrations: 487 nm ( $17600 \text{ M}^{-1} \text{ cm}^{-1}$ ), 538 nm ( $8250 \text{ M}^{-1} \text{ cm}^{-1}$ ), and 565 nm ( $10500 \text{ M}^{-1} \text{ cm}^{-1}$ ). The  $\epsilon$  values at the same wavelengths for (TMP)Fe<sup>II</sup> were also used: 487 nm ( $5720 \text{ M}^{-1} \text{ cm}^{-1}$ ), 538 nm ( $11600 \text{ M}^{-1} \text{ cm}^{-1}$ ), and 565 nm ( $5670 \text{ M}^{-1} \text{ cm}^{-1}$ ). Although there was a slight temperature dependence on these values (~5%), it was assumed that they were effectively constant over the temperature range from which they were taken (5°C to 75°C). A larger error is reported to compensate for this simplification. The absorption of free TEMPO was negligible within the error of the measurements [TEMPO  $\lambda_{\max}$  (MeCN) = 460 nm ( $10.3 \text{ M}^{-1} \text{ cm}^{-1}$ )<sup>7</sup>].

At each temperature,  $K_4$  was determined from the optical spectrum at the three wavelengths mentioned using the following equations derived from mass balance assumptions (the 1 cm pathlength term is not included):

$$[\text{Fe}^{\text{II}}] = (\text{A}_{\text{obs}} - \epsilon_{\text{Fe(III)}}[\text{Fe}^{\text{II}}_0]) / (\epsilon_{\text{Fe(II)}} - \epsilon_{\text{Fe(III)}})$$

$$[\text{Fe}^{\text{III}}] = [\text{Fe}^{\text{II}}_0] - [\text{Fe}^{\text{II}}]$$

$$[\text{TEMPO}] = [\text{TEMPO}_0] - [\text{Fe}^{\text{III}}]$$

$$K_4 = [\text{Fe}^{\text{III}}] / [\text{Fe}^{\text{II}}][\text{TEMPO}]$$

Where  $[\text{Fe}^{\text{II}}$ ] is the equilibrium concentration of (TMP) Fe<sup>II</sup>,  $\text{A}_{\text{obs}}$  is the observed absorbance,  $\epsilon_{\text{Fe(III)}}$  is the epsilon value of (TMP)Fe<sup>III</sup>(TEMPO),  $\epsilon_{\text{Fe(II)}}$  is the epsilon value of (TMP)Fe<sup>II</sup>,  $[\text{Fe}^{\text{II}}_0]$  is the initial concentration of (TMP)Fe<sup>II</sup>,  $[\text{TEMPO}]$  is the equilibrium concentration of TEMPO, and  $[\text{TEMPO}_0]$  is the initial concentration of TEMPO.

| Temperature (°C) | $K_4 (M^{-1})$ |
|------------------|----------------|
| 5                | 1120           |
| -5               | 1900           |
| -15              | 3440           |
| -25              | 6320           |
| -35              | 12000          |
| -45              | 24400          |
| -55              | 41000          |
| -65              | 85700          |
| -75              | 210000         |

Plotting  $\ln(K_4)$  vs.  $1/T$  shows a linear relationship. The values of  $\Delta H^\circ$  and  $\Delta S^\circ$  were determined by applying the van't Hoff equation:

$$\ln(K_4) = -(\Delta H^\circ/RT) + (\Delta S^\circ/R)$$

(7) A. Wu, E. A. Mader, A. Datta, D. A. Hrovat, J. M. Mayer, *J. Am. Chem. Soc.* 2009, **131**, 11985.

## 7. Decoalescence of (TMP)Fe<sup>III</sup>(TEMPO) *m*-aryl peaks in variable temperature NMR spectra.

In a J. Young NMR tube one equivalent of TEMPO was added to a 4 mM solution of (TMP)Fe<sup>II</sup> in toluene-*d*<sub>8</sub>. Over the temperature range used, 237 K to 224 K, equilibrium 4 lies nearly completely on the side of (TMP)Fe<sup>III</sup>(TEMPO) with equilibrium concentrations ranging from 3.98 to 3.99 mM or 99.5 to 99.8%.

For each spectrum acquired, the sample was allowed to reach thermal equilibrium for 5 minutes prior to collecting data.

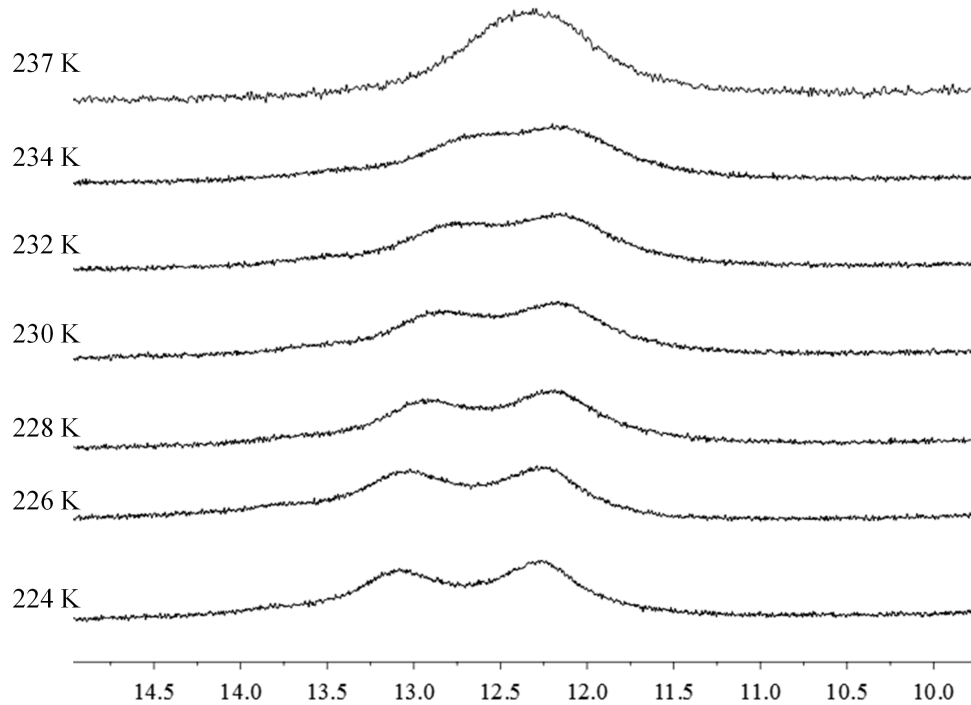


Figure S6. Decoalescence of the *m*-aryl resonances of (TMP)Fe<sup>III</sup>(TEMPO) occurs with decreasing temperature.

Based on these spectra, the difference in chemical shift of the coalescing peaks is about 0.8 ppm, or 500 Hz, and the coalescence temperature is about 235 K. There is some uncertainty in these estimates because the temperature dependence of the paramagnetic chemical shifts is not being

taken into account, but this will not cause a large error over this narrow temperature range. The rate constant at the coalescence temperature is given by:

$$k = \Delta v (\pi / \sqrt{2})$$

which is  $1100 \pm 200 \text{ s}^{-1}$ .

Inserting this value into the Eyring equation gives  $\Delta G^\ddagger = RT \ln(k \times k_B T / h) = 16.9 \pm 0.5 \text{ kcal mol}^{-1}$  at 235 K.

### 8. $^1\text{H}$ NMR spectrum of (TMP)Fe<sup>II</sup> + substoichiometric TEMPO at -80 °C.

The resonances for both (TMP)Fe<sup>II</sup> ( $\times$ ) and (TMP)Fe<sup>III</sup>(TEMPO) ( $\bullet$ ) can be observed at -80 °C when substoichiometric TEMPO is added to (TMP)Fe<sup>II</sup> in toluene- $d_8$ .

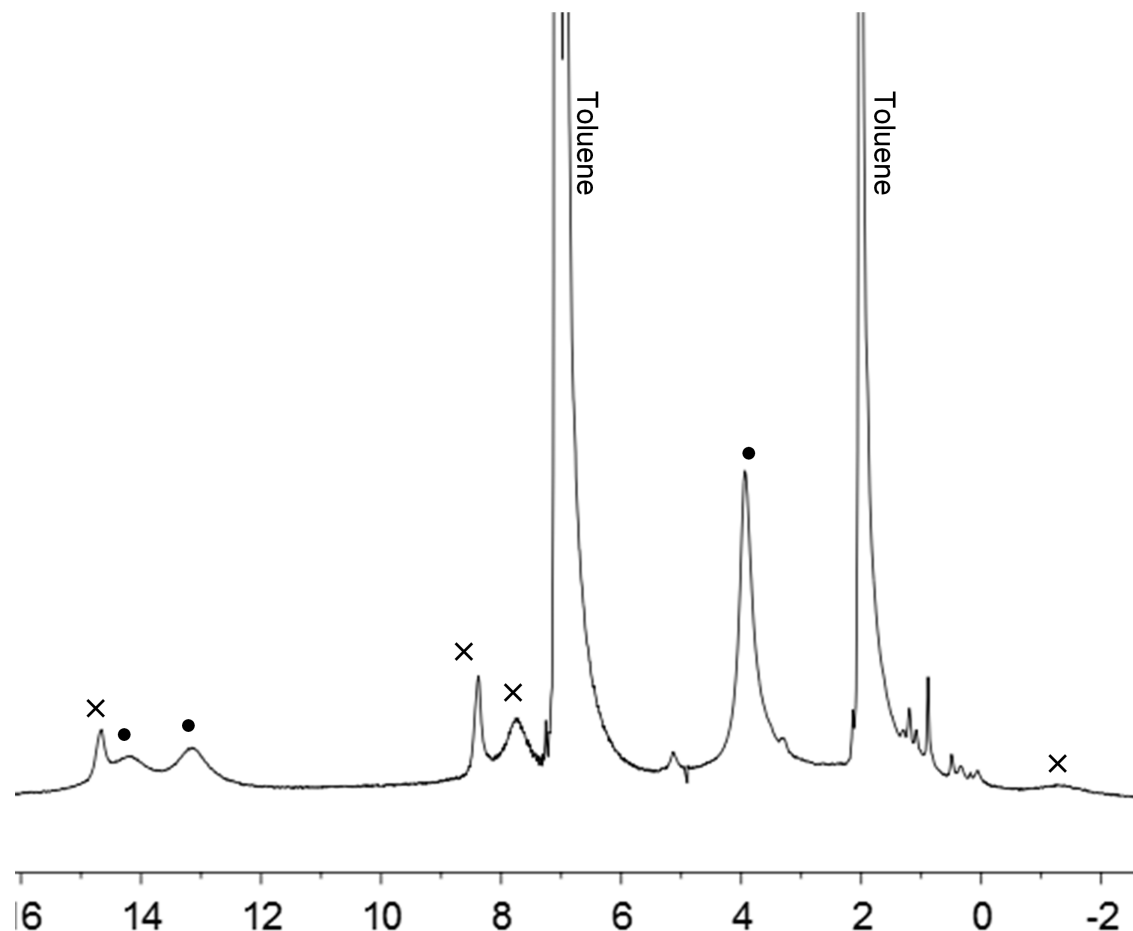


Figure S7.  $^1\text{H}$  NMR spectrum of (TMP)Fe<sup>II</sup> + substoichiometric TEMPO in toluene- $d_8$  at -80 °C. At low temperatures, the resonances for (TMP)Fe<sup>II</sup> ( $\times$ ) and (TMP)Fe<sup>III</sup>(TEMPO) ( $\bullet$ ) are distinguishable.

9.  $^1\text{H}$  NMR spectrum of (TMP)Fe<sup>II</sup> +  $^t\text{Bu}_3\text{ArO}\cdot$

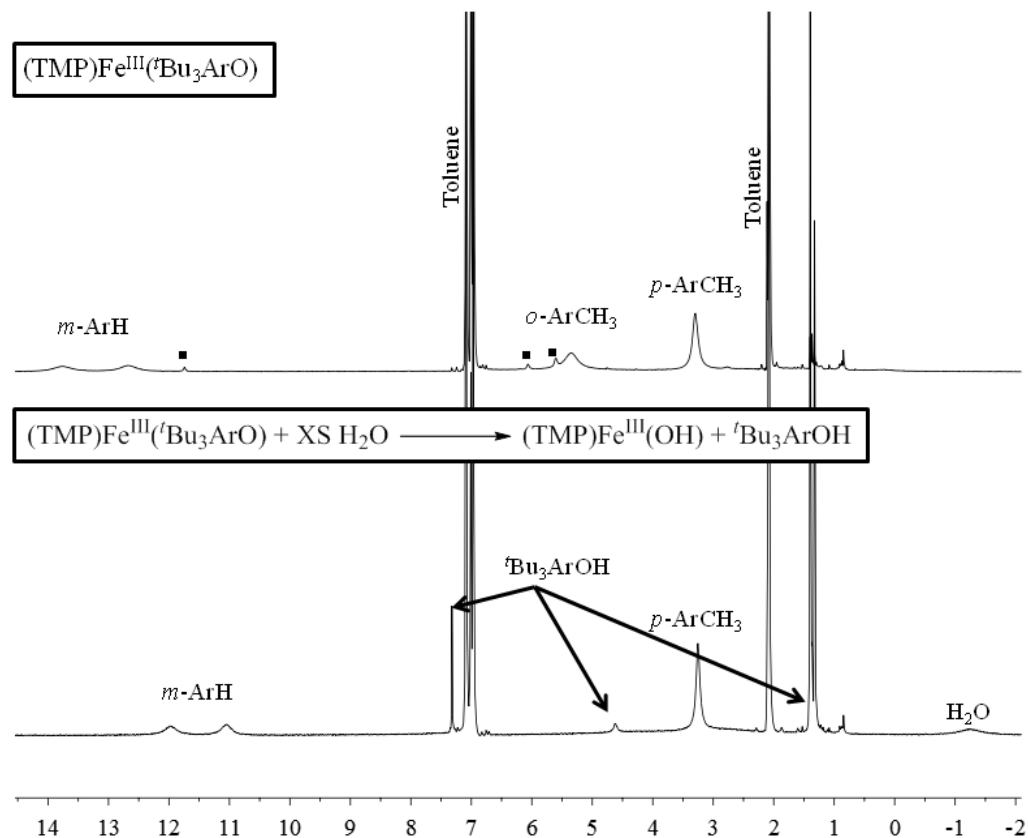


Figure S8.  $^1\text{H}$  NMR spectra of (TMP)Fe<sup>III</sup>( $^t\text{Bu}_3\text{ArO}$ ) in toluene- $d_8$  (top) and (TMP)Fe<sup>III</sup>( $^t\text{Bu}_3\text{ArO}$ ) plus excess degassed H<sub>2</sub>O in toluene- $d_8$  (bottom). The broad  $\beta$ -pyrrolic resonances are not shown. In the top spectrum, a small amount of (TMP)Fe<sup>II</sup> impurity is present (■).

**10.  $^1\text{H}$  NMR spectrum of (TMP)Fe<sup>II</sup> + TEMPOH**

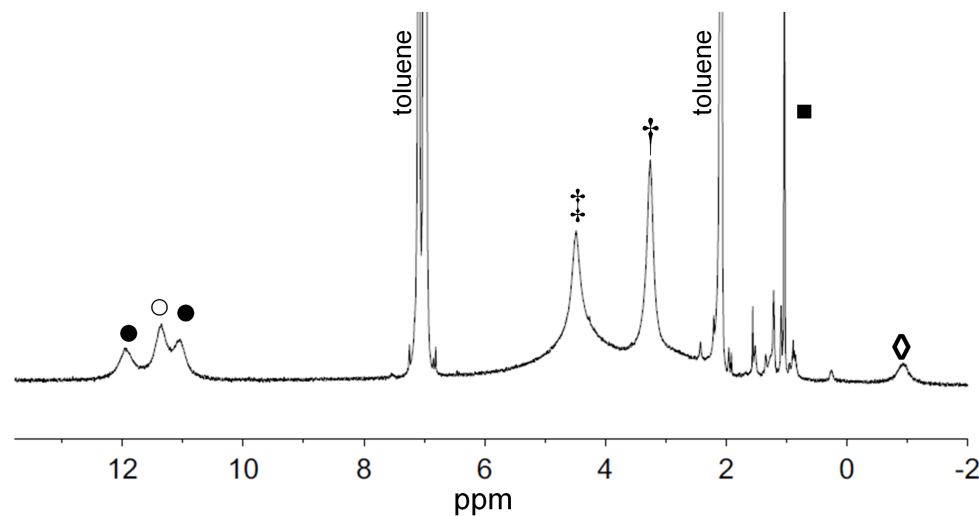


Figure S9.  $^1\text{H}$  NMR spectrum of the reaction mixture of 4.0 mM (TMP)Fe<sup>II</sup> with one equivalent of TEMPO-H in toluene- $d_8$  after 12 hours: (TMP)Fe<sup>III</sup>(OH) *p*-CH<sub>3</sub> peak (†) and *m*-Ar peaks (•), (TMP)Fe<sup>III</sup>(TEMPO)/(TMP)Fe<sup>II</sup> complex *p*-CH<sub>3</sub> peak (‡) and *m*-Ar peak (○), TEMP-H peaks (■), and H<sub>2</sub>O. The broad overlapping downfield B-pyrrolic signals for (TMP)Fe<sup>III</sup>(OH) (~81 ppm) and (TMP)Fe<sup>III</sup>(TEMPO)/(TMP)Fe<sup>II</sup> (~45 ppm) are not shown.

**11.  $^1\text{H}$  NMR spectrum of (TMP)Fe<sup>II</sup> + 2 TEMPOH**

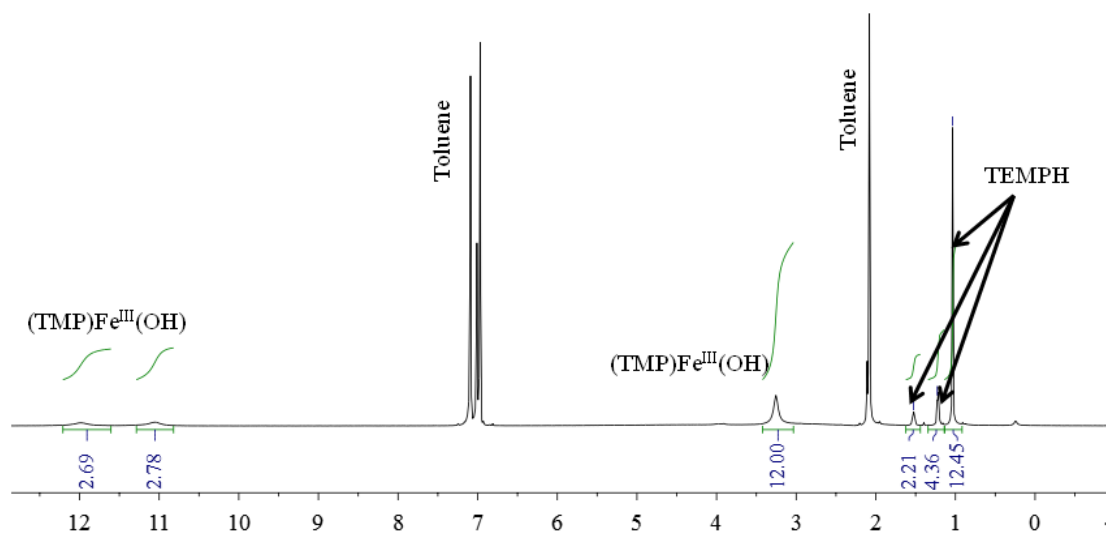


Figure S10.  $^1\text{H}$  NMR spectrum of the products of the reaction between (TMP)Fe<sup>II</sup> and 2 equivalents of TEMPOH in toluene- $d_8$ . The integrations indicate the reaction generates one equivalent of (TMP)Fe<sup>III</sup>(OH), one equivalent of TEMPH. Presumably one equivalent of NMR-silent TEMPO is generated as well.

## 12. Kinetic data for the catalytic disproportionation of TEMPOH in the presence of catalytic (TMP)Fe<sup>II</sup>

The catalytic disproportionation of TEMPOH was monitored by <sup>1</sup>H NMR on a Bruker 500 MHz spectrometer by taking a single scan every 10 minutes for 500 minutes. Samples were prepared in a nitrogen filled glovebox in which a benzene-*d*<sub>6</sub> solution containing (TMP)Fe<sup>II</sup> (40 μM) and TEMPOH (5.0 mM) was prepared and frozen in a -78°C coldwell before mixing could occur and thawed immediately before time-based measurements were taken. All spectra were phased and integrated identically using MestReNova. Concentrations of TEMPOH and TEMPH were determined by comparing their integrations to the integration of a known concentration of hexamethylbenzene.

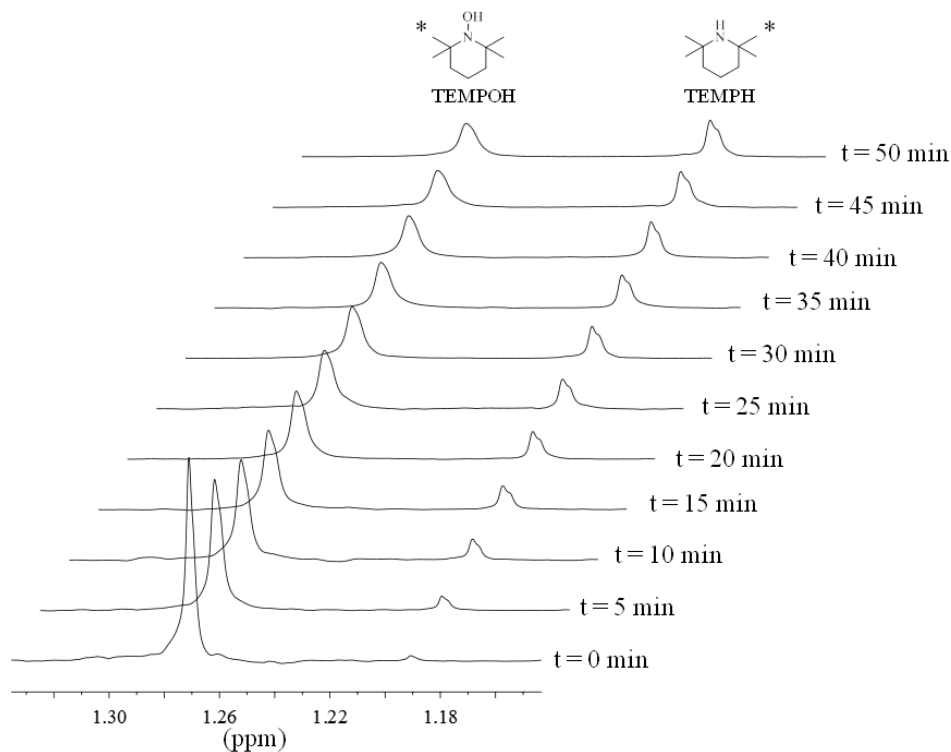


Figure S11. Selected <sup>1</sup>H NMR slices of the decomposition of TEMPOH in the presence of a catalytic amount of (TMP)Fe<sup>II</sup>.

**13. Mass balance plot for the disproportionation of TEMPOH in the presence of catalytic (TMP)Fe<sup>II</sup>**

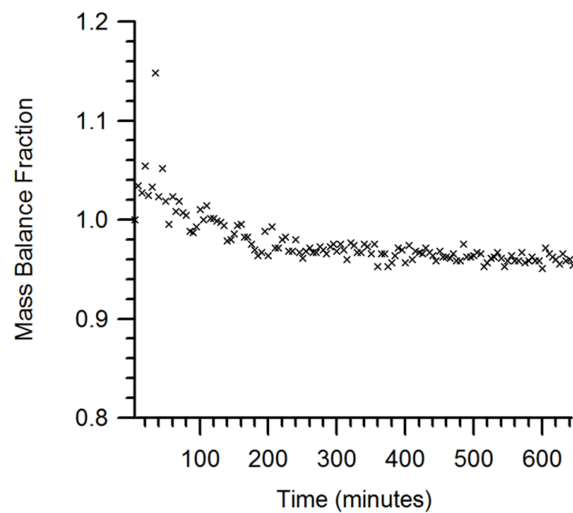


Figure S12. Mass balance plot for the catalytic disproportionation of TEMPOH. Mass balance fraction describes the observed amount of TEMP-H generated in relation to the amount of observed TEMPOH consumed. A mass balance fraction equal to 1 would describe perfect mass balance in which one TEMP-H was generated for every 3 TEMPOH consumed.

Using the data in Figure S11, mass balance was calculated using the following equation based on the reaction stoichiometry:

$$F(t) = ([\text{TEMPH}]_t + [\text{TEMPO}]_t + [\text{TEMPOH}]_t)/[\text{TEMPOH}]_0$$

Where  $t$  is time,  $[\text{TEMPH}]_t$  is the concentration of TEMP-H at time  $t$ ,  $[\text{TEMPOH}]_t$  is the concentration of TEMPOH at time  $t$ ,  $[\text{TEMPO}]_t$  is the concentration of TEMPO at time  $t$  (taken to be  $= 2 \times [\text{TEMPH}]_t$ ) and  $[\text{TEMPOH}]_0$  is the concentration of TEMPOH at  $t = 0$ .

#### 14. Experimental details for the treatment of (TMP)Fe<sup>III</sup>(OH) with excess P1-phosphazeneH<sup>+</sup>BF<sub>4</sub><sup>-</sup>

In a J. Young NMR tube, 20 equivalents of *tert*-butylimino-tris(pyrolidino)phosphorane hydrofluoroborate, P1-phosphazeneH<sup>+</sup>BF<sub>4</sub><sup>-</sup>, was added to a 6.6 mM solution of (TMP)Fe<sup>III</sup>(OH) in dichloromethane-*d*<sub>2</sub>. No reaction was observed by <sup>1</sup>H NMR after 1 h.